Energy &
Environmental Science

Dynamic Article Links

Cite this: *Energy Environ. Sci.*, 2011, **4**, 751

www.rsc.org/ees

PAPER

Water and ion transport through functionalised carbon nanotubes: implications for desalination technology

Ben Corry*

Received 27th September 2010, Accepted 10th December 2010
DOI: 10.1039/c0ee00481b

The use of semipermeable membranes containing carbon nanotubes (CNTs) that form continuous pores has been suggested as a way to reduce the cost of desalination *via* reverse osmosis. Example membranes containing aligned CNTs have been fabricated, but obtaining only the very narrow pores that are able to block the passage of ions while allowing a rapid flow of water remains a challenge and previous computational studies have focused on idealised tubes. Here molecular dynamics simulations are used to examine water and ion transport through functionalised CNTs with the aim of investigating whether such chemical modification allows the performance of CNT based membranes to be improved, or for larger diameter pores to be used. A range of different charged and polar functional groups were added to a 1.1 nm diameter (8,8) CNT that was previously found to be only moderately effective at rejecting ions. These CNTs were incorporated into membranes and simulations were conducted with a hydrostatic pressure difference to determine the ion rejection and flux of water passing through each as well as the energy barriers presented to ions and water molecules. The results show that the addition of charges at the entrance of the pore can help to prevent the passage of ions, however, any functionalisation also reduces the flow of water through the membrane due to increased electrostatic interactions between the water molecules and the CNT. Assuming pore densities that have previously been achieved, the performance of these membranes in the simulations is still many times better than existing technology and thus the inclusion of functionalised CNTs in desalination membranes may prove to be useful in achieving salt rejection and rapid water flow.

1 Introduction

Although much of the earth is covered in water, most of this is either too salty for human consumption and agriculture or is locked up in ice and snow.[1] As a consequence, many people face difficulties in accessing fresh water and currently nearly one in eight lack access to clean reliable water supplies.[2] Addressing this problem is difficult as the growing world population and escalating levels of agriculture and industry mean that demands on fresh water are likely to increase. In addition, climatic changes are predicted to alter the natural availability of non-saline water, resulting in both shifts in the location of available water and creating greater uncertainty in fresh water supplies.[3] The

School of Biomedical, Biomolecular and Chemical Sciences, The University of Western Australia, Perth, Australia. E-mail: ben.corry@uwa.edu.au

Broader context

Increasing strain is being put on world fresh water supplies due to growth in population, industry and agriculture as well as climatic shifts. Thus, many communities are turning to the desalination of salty or brackish water to meet their needs. However, this process requires large amounts of energy and is a costly means of obtaining clean water. One way to make this technology more efficient is to create new semipermeable membranes for reverse osmosis systems that allow a greater flow of water while blocking salts. Pioneering experimental and computational studies have suggested that membranes containing continuous pores formed from carbon nanotubes may be able to achieve this goal, but fabricating such a membrane that can both rapidly transport water but block salts has yet to be achieved. Here we move away from the idealised models used in previous computational studies and examine how chemical modification of the nanotubes affects their suitability for desalination. Although the flow of water in such tubes found in our simulations is less than in unmodified pores it is still many times larger than commercial reverse osmosis membranes. Furthermore, the appropriate choice of functionalisation can improve salt rejection and allow larger diameter pores to be used than has previously been thought.

desalination of salty water provides one way of boosting fresh water supplies and although it currently accounts for only 0.5% of all water supply[2] it is likely to become increasingly important. In most cases, the cost of obtaining fresh water from desalination is greater than from other sources, so one of the main challenges in making this technology more practical is to find ways of making it cheaper.

Currently, the most common method for desalinating water is 'reverse osmosis' in which salty water is put under high pressure to force it through semipermeable membranes that allow the passage of water but block ions. Improvements in these polymer based membranes that have allowed a greater flux of water while still preventing the passage of salts, have been largely responsible for the decreasing cost of desalinated water over the last 20 years, but further improvement is still required to make this technology widespread. Recently it has been proposed that such membranes could be further significantly improved *via* the inclusion of continuous smooth pores that could allow much greater water flow while still rejecting ions.

The somewhat surprising finding in simulation studies that water can enter narrow hydrophobic channels such as the interior of carbon nanotubes (CNTs)[4,5] has been confirmed experimentally,[6,7] opening the door to the inclusion of CNTs into membranes to form smooth pores for the purpose of desalination. Recent advances in fabrication techniques have allowed aligned CNTs to be arranged within membranes and for the transport of water and gases through these membranes to be observed.[8–10] A surprising feature is that the flux of water and gases through these membranes has been considerably higher than expectations derived from continuum hydrodynamic theories, something also observed in the simulations.[4,5,11] Selective gas transport[9] and subsequently ion rejection in low concentration solutions[12] have been observed in membranes containing sub-2nm diameter pores. However, the ion rejection was lost at higher concentrations such as would be required for desalinating sea water. The rapid water flux that has been observed in these CNT containing membranes suggests that they would provide an ideal basis for desalination membranes if salt rejection could also be achieved.

Simulation studies on non-polar model pores,[13–15] mechanosensitive channels[16,17] and acetylcholine receptors[18,19] indicate that there is a critical diameter for non-polar pores above which water will pass but below which it will not. Near this diameter it is possible that ions will be blocked while water continues to pass. Recent simulations have studied water and ion transport through CNTs with a range of diameters finding that there is a range of pore sizes through which water passes rapidly but ions do not[20] and have shown that the degree of selectivity towards different ion types varies with pore radius,[21] thus demonstrating the potential for these membranes to improve desalination technology. Indeed, the large water fluxes seen in these simulations give hope to the aim of significantly reducing the cost of desalination *via* reverse osmosis with CNT based membranes. However, these simulations also suggest that very narrow CNTs with diameters less than 1 nm are required to achieve sufficient salt rejection. The ability to fabricate membranes containing only tubes of this diameter remains a substantial challenge. While it is the non-polar nature of the CNTs that appears to make them suitable for use in desalination membranes, simulations have also suggested that nanotubes formed from other materials, such as boron nitride may also be suitable.[22]

The importance of pore size in determining water flux and salt rejection has been investigated in simulations, but it remains to be seen if chemical modification of the pores could improve their performance. Furthermore, it is doubtful whether the ideal unfunctionalised CNTS that have previously been studied in simulations exist in reality, as opening the ends of the CNTs usually imparts some kind of chemical modification. Thus, it is critical to see how such modification influences the salt rejection and water permeation through the pores in order to know if this technology can become a reality. The aim of this manuscript is to start to address these issues and also to see if wider pores could be used if appropriately functionalised. Experimental studies have been conducted to see how transport of large cations through wider 7 nm diameter CNTs is influenced by tip-functionalisation using charged or bulky groups.[23] Here the focus is on smaller diameter pores that are more likely to be useful in removing small salts from water, taking a CNT of a size that was found to be only moderately successful at blocking ions in previous simulations. Molecular dynamics simulations are used to investigate whether the addition of small charged or polar functional groups can increase the level of salt rejection without significantly decreasing water flux.

2 Methods

Membranes composed of carbon nanotubes were modelled following our previous methodology[20,21] based on that of Zhu and Schulten[24] in which 12 (8,8) armchair type carbon nanotubes, each 10.9 Å in diameter (measured between carbon centres) and 13 Å long are hexagonally packed as shown in Fig. 1. Periodic boundaries were employed to form a continuous 2-D membrane that was solvated by ~30 Å thick layers of TIP3P water on either side with Na^+ and Cl^- randomly placed to both neutralise the system and yield a net concentration of 200 mM NaCl. Four types of functional groups (carboxylate anion COO^-, amine cation NH_3^+, hydroxyl OH and amide $CONH_2$, Fig. 2) were added to either one or three CNTs in the simulation using parameters from the CHARMM27 force field.[25] Either 4 or 8 functional groups were added at positions spread uniformly around the top rim of the CNT. Following Hummer *et al.*[4,5] and our previous work[20,21] all carbon atoms not in the functional groups were taken to be neutral with force field parameters taken as those for aromatic carbons (CA) in the CHARMM27 parameter set. Before collecting data, all systems were energy minimised and equilibrated for 0.5 ns under a constant pressure of 1 atm and temperature of 300 K during which time a harmonic constraint applied to the carbon atoms was gradually reduced from 1 kcal mol^{-1} $Å^{-2}$ to 0.1 kcal mol^{-1} $Å^{-2}$. After this, harmonic restraints of 0.1 kcal mol^{-1} $Å^{-2}$ were applied to all the carbon atoms not part of the functional groups to keep the membrane roughly in place.

To gain results, two main types of simulations methodology were employed to (i) examine transport under hydrostatic pressure conditions and (ii) to determine the free energy barriers to ion and water permeation through the tubes. To achieve the first aim, a method developed by Zhu *et al.* was employed to introduce a hydrostatic pressure difference across the membrane.[26,27]

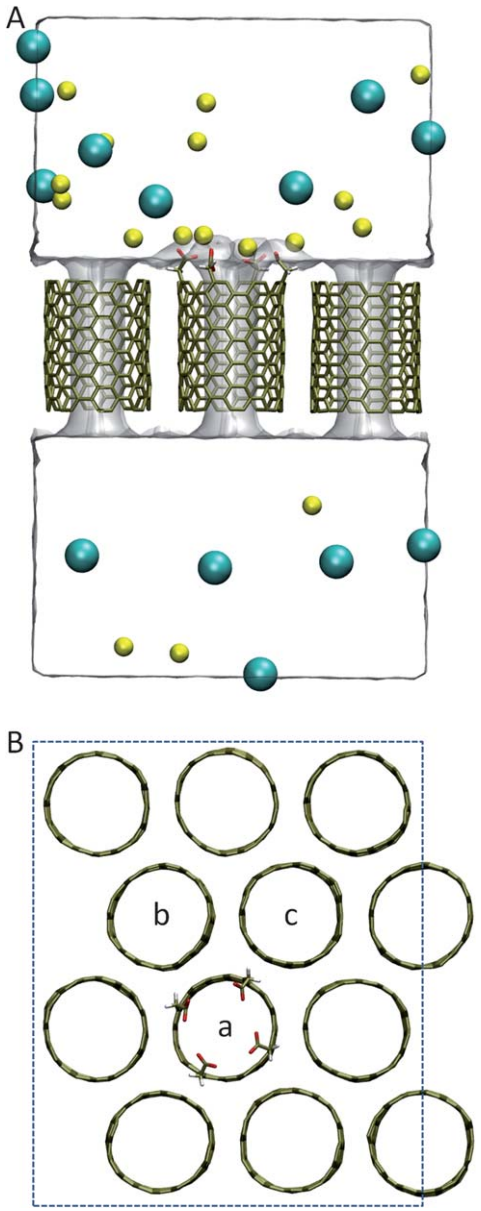

Fig. 1 Simulation system. (A) A slice through the simulation system showing 3 of the 12 CNTs (brown). The edge of the periodic box is shown as are Na^+ (yellow) and Cl^- (blue). In this case the central CNT is functionalised with 4 COO^- groups. Due to the periodic nature of the simulation, ions that move out one side of the system enter from the opposite side. (B) The arrangement of CNTs viewed from above the plane of the membrane. The edge of periodic simulation system is showm by the dotted line. Most simulations are conducted functionalising only one of the CNTs (labelled a) as shown, while in 2 cases the tubes labelled b and c are also functionalised.

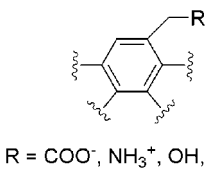

Fig. 2 The different functional groups that are examined are shown.

In this, a constant force f in the direction perpendicular to the plane of the membrane is applied to water molecules in layers at the very top and bottom of the simulation system. Due to the periodic nature of the simulation this creates a region of water at high pressure on one side of the membrane and lower pressure on the opposite side with the total pressure difference given by $\Delta P = nfl/A$, where n is the number of water molecules in the section to which forces are applied and A is the cross sectional area of the membrane.[26] In this case, forces were applied to water in a 16 Å thick layer defined by those molecules greater than 19 Å from each side of the membrane. Simulations involving hydrostatic pressure differences were performed under constant volume and constant temperature (300 K) conditions using a Langevin thermostat. Errors were obtained from the standard deviation found when breaking each simulation into 20 parts each lasting 2ns.

In the second type of simulations, umbrella sampling[28] was used to determine the 2 dimensional potential of mean force (PMF) in the axial and radial directions for ions and water in and around the nanotubes in an NPT ensemble. In this method a harmonic biasing potential $\frac{K_r}{2}(r-r_i)^2+\frac{K_z}{2}(z-z_i)^2$ was applied to a molecule where r and z are the radial and axial coordinates of the ion defined from the centre of one of the pore, r_i and z_i are target ion positions and K_r and K_z are corresponding force constants. In contrast to our previous simulations of unfunctionalised CNTs, it was found that greater sampling was required to accurately determine the PMF at the entrance to the pores near the location of the functional groups where the forces can be quite large, especially when charged groups were used that can attract multiple ions. To achieve this greater level of conformational sampling, three types of bias potentials were used. The first covered the full length of the pore (from $z = -12$ to $z = 12$) and had target positions separated by 0.5 Å in the z direction for both $r = 0$ and $r = 5$ with force constants of $K_r = 0.1$ and $K_z = 1.0$ kcal mol^{-1} Å^2. The second was used to better sample positions close to the pore axis and involved positions separated by 1 Å in the z direction at $r = 0$ with force constants of $K_r = 3.0$ and $K_z = 3.0$ kcal mol^{-1} Å^2. Finally, an additional set of biases was used around the functionalised mouth of the pore with $-1.5 < z < 10.5$ and $0 < r < 5.0$ with force constants of $K_r = 5.0$ and $K_z = 5.0$ kcal mol^{-1} Å^2 and a 1 Å spacing in both directions. Collective analysis of the data was made using the weighted histogram analysis method[29,30] using the implementation of Grossfield[31] taking account of the changing size of the volume element in the r direction. One dimensional PMFs were obtained by integrating the normalised probabilities in the $x-y$ plane up to $r = 5$ Å.

Simulations were conducted with NAMD 2.7[32] with a 1 fs time step using a 12 Å cutoff for van der Waals interactions and a particle mesh Ewald scheme for electrostatic calculations.

3 Results and discussion

3.1 Transport in unfunctionalised CNTs

Before looking at the various functionalised CNTs it is worth briefly revisiting the mechanisms of transport and rejection in the

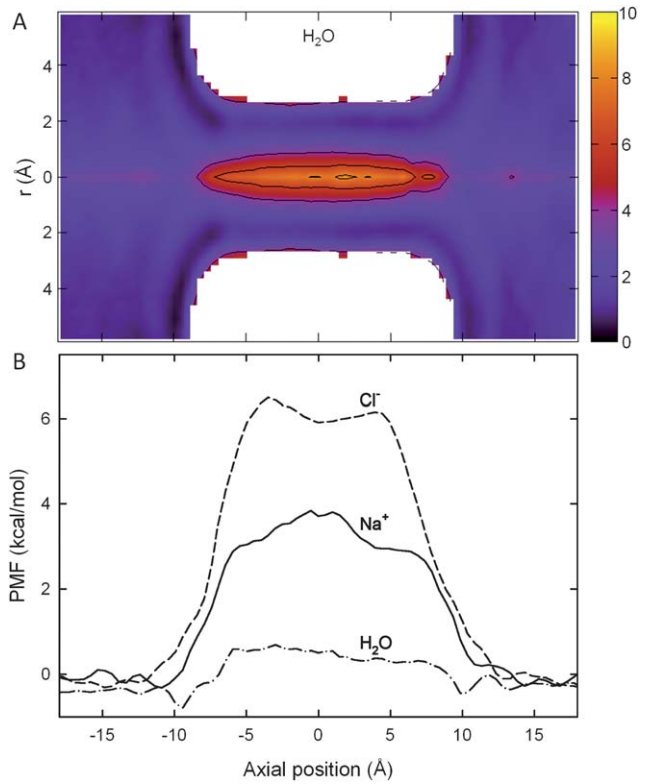

Fig. 3 Potential of mean force in an unfunctionalised (8,8) CNT. (A) The two dimension PMF for water in the CNT. (B) The PMF in the axial direction of the pore for water, Na^+ and Cl^-.

unfunctionalised (8,8) CNT. In these and previous simulations,[20,21] water readily enters the tube forming four relatively stable interconnected water chains that span the length of the pore (see Fig. 2 in[20]). Interestingly, because of this four chain arrangement, water oxygens almost never reside on the pore axis as can be seen when plotting the 2D PMF shown in Fig. 3A. It is also notable in the PMF that there is almost no energy barrier for water to move through the pore in the off-axis positions, and as a result the flux of water through the unfunctionalised (8,8) CNTs is large as shown in Table 1. The water flux value is converted to more conventional macroscopic units in Table 2. The flux of water passing through the pore (and salt rejection) is expected to be largely length independent as the interior of the pores is smooth and relatively frictionless and most of the energy barriers are encountered at the entry and exit of the channels.[5,20]

Under hydrostatic pressure, Na^+ is also found to pass through the (8,8) CNTs pores. Due to its small size, it can sit in an axial position in the pore surrounded by most of its first solvation shell (five or more water molecules) and as a consequence there is only a small energy penalty for Na^+ entry of less than 4 kcal mol^{-1} (Fig. 3B and[21]). The larger Cl^- can also fit into the pore surrounded by up to six water molecules in an off axis position, but due to its large bulk and consequent inability to fit as much of its solvation shell into the pore it suffers a slightly greater dehydration penalty upon entry of close to 6 kcal mol^{-1}. The ability of the nanotubes to reject salt can be quantified from the ratio of the number of each type of ion passing through the pores to the number of water molecules passing through the pores and comparing this to the ratio of ions to water in the simulation system as a whole. As expected from the greater energy barriers presented to ions than to water the (8,8) does partly succeed in rejecting the ions, but not to the extent that is required to make sea water potable (around 95% rejection) as shown in Table 1. Due to the larger dehydration barrier faced by Cl^-, the rejection of Cl^- is greater than that of Na^+. In our simulations the upstream and downstream reservoirs are connected through the periodic boundary which prevents charge separation arising from the differential rejection of Cl^- and Na^+. In a system in which the two reservoirs are not connected or there is not a high flow past the membrane, such charge separation could be expected to equalise the rejection of the two ion species.

3.2 Water transport in functionalised CNTs

To see if the addition of charged or polar groups at the ends of the CNTs can improve their potential for desalination these simulations were repeated on CNTs functionalised by a range of charged and polar groups shown in Fig. 2. The key results are summarised in Table 1, with flux values converted to more conventional units in Table 2.

Table 1 Water flux and ion rejection through functionalised carbon nanotubes under a hydrostatic pressure difference of 246 MPa. All flux values are in number of molecules per tube per ns and are calculated from 40 ns of simulation. The % water flux is that passing through the functionalised CNT compared to the average of that passing through the unfunctionalised CNTs from the same simulation. The result labelled 3 × ($2NH_3^+$) represents a simulation containing 3 functionalised CNTs, each with $2NH_3^+$ groups

Tube type	Water flux	% Water flux	Na^+ flux	Cl^- flux	Na^+ rejection	Cl^- rejection
non func	107.8 ± 0.6	100%	0.22 ± 0.01	0.05 ± 0.01	28%	86%
$4COO^-$	35 ± 2	33%	0.10 ± 0.04	0.00 ± 0.03	32%	100%
$8COO^-$	14 ± 3	13%	0.00 ± 0.03	0.00 ± 0.03	100%	100%
$2NH_3^+$	60 ± 2	67%	0.03 ± 0.03	0.03 ± 0.03	86%	87%
$4NH_3^+$	22.1 ± 0.7	24%	0.00 ± 0.03	0.00 ± 0.03	100%	100%
$8NH_3^+$	18.9 ± 0.8	18%	0.00 ± 0.03	0.03 ± 0.03	100%	66%
$2NH_3^+$ $2COO^-$	46 ± 2	49%	0.03 ± 0.03	0.03 ± 0.03	82%	82%
$4NH_3^+$ $4COO^-$	18 ± 1	17%	0.03 ± 0.03	0.00 ± 0.03	55%	100%
4OH	70 ± 2	75%	0.30 ± 0.06	0.10 ± 0.06	−16%	61%
8OH	43 ± 2	47%	0.08 ± 0.04	0.00 ± 0.03	50%	100%
$4CONH_2$	59 ± 3	65%	0.13 ± 0.06	0.03 ± 0.03	41%	86%
$8CONH_2$	38 ± 2	42%	0.10 ± 0.04	0.00 ± 0.03	29%	100%
3 × ($2NH_3^+$)	59 ± 1	66%	0.01 ± 0.01	0.02 ± 0.01	94%	92%
3 × ($4NH_3^+$)	23 ± 1	25%	0.00 ± 0.01	0.00 ± 0.01	100%	100%

Table 2 Water flux through functionalised carbon nanotubes membranes in macroscopic units. Values are given assuming the theoretical maximum pore density and a pore density that has previously been achieved.[9] Reported permeate flow for a FilmTech SW30HR-380 reverse osmosis membrane[35] is given for comparison. A crude decision is given as to whether each CNT is achieving the salt rejection required to make sea water potable, with ~ representing those that are near the desired value

	Water flux ($\times 10^{-12}$ m s^{-1}Pa^{-1})		
Tube type	Maximal pore density 5.8×10^{17} pores m^{-2}	Achieved pore density 2.5×10^{15} pores m^{-2}	Desired salt rejection achieved?
non func	7580	32.7	N
4COO$^-$	2460	10.6	N
8COO$^-$	990	4.2	Y
2NH$_3^+$	4240	18.3	~
4NH$_3^+$	1550	6.7	Y
8NH$_3^+$	1330	5.7	N
2NH$_3^+$ 2COO$^-$	3240	13.9	~
4NH$_3^+$ 4COO$^-$	1270	5.5	N
4OH	4920	21.2	N
8OH	3020	13.0	N
4CONH$_2$	4150	17.9	N
8CONH$_2$	2670	11.5	N
3 × (2NH$_3^+$)	4470	19.3	Y
3 × (4NH$_3^+$)	1740	7.5	Y
SW30HR-380		1.4	

The first notable aspect of these data is that the flux of water through the pores is smaller in all the functionalised tubes compared to the non-functionalised case. As the effective pressure in the simulations depends upon the number of water molecules in the region to which forces are applied, the size of the simulation system and any osmotic gradients that develop, it does vary slightly between simulations, but the difference is estimated to be less than a few MPa. As each simulation contains 11 unfunctionalised CNTs and one functionalised CNT, the flux through the non-functionalised CNTs in each simulation (Table 3) can be used as an internal control and the percentage flux passing through the functionalised tube compared to that passing through the unfunctionalised tubes is reported in Table 1. The reduced water flux in the functionalised tubes, can, therefore be soundly attributed to different transport characteristics in these CNTs.

The reduction in water flux can be attributed to two different phenomena. The first of these arises from steric blockages of the pore by either the functional groups themselves or by ions that are strongly attracted to them. This is most notable for the tube containing eight COO$^-$ groups depicted in Fig. 4A, in which an average of four (Table 4) and as many as eight ions cluster around the pore entrance. The consequence of this is that the effective area through which water molecules can pass is reduced, as is clearly seen in the plot of water concentration in the pore Fig. 5A and hence the water conductance decreases. This phenomenom arises to a greater extent as the pores become more highly charged, but is likely to be less important in the pores containing polar rather than charged groups where ions do not permanently reside near the pore entrance.

A more general reason for the decreased water flux is the introduction of significant direct interactions between the water molecules and the functional groups as shown in Fig. 5B. Whereas water forms only weak van der Waals interactions with the uncharged carbon atoms in the CNT core, much stronger and more localised electrostatic interactions can arise with the charged or polar gatekeepers. A consequence of these interactions is that water molecules temporarily pause to reside in favoured positions near the functional groups, as can be seen in the clearly defined structure of water inside the pore depicted in Fig. 5A. As a consequence of there being preferred positions near the mouth of the pore, a series of concentration peaks can be observed throughout the pore, each separated by the size of one water molecule. More importantly, the longer each water molecule spends bound at the channel mouth, the more it slows the passage of all water molecules through the pore. Both the time spent at the channel mouth and the transit time are increased. Altering the smooth neutral surface of the pore removes the conditions for the rapid 'non-slip' flow seen in the unfunctionalised CNTs, creating friction to the passage of water.

3.3. Ion rejection in functionalised CNTs

While functionalising the CNTs reduces the flux of water through the pores, in many cases it also improves the salt rejection. The inclusion of charged groups influences the rejection of both the like and oppositely charged ions. As can be seen in

Table 3 Water flux and ion rejection through the unfunctionalised tubes in each simulation under a hydrostatic pressure of ~246 MPa. All flux values are in number of molecules per tube per ns

Tube type	Water flux	Na$^+$ flux	Cl$^-$ flux	Na$^+$ rejection	Cl$^-$rejection
non func	107.8 ± 0.7	0.22 ± 0.01	0.05 ± 0.01	28%	86%
4COO$^-$	105.5 ± 0.3	0.26 ± 0.01	0.04 ± 0.01	42%	88%
8COO$^-$	107.1 ± 0.7	0.23 ± 0.02	0.03 ± 0.01	55%	90%
2NH3$^+$	89.0 ± 0.3	0.18 ± 0.01	0.03 ± 0.01	42%	91%
4NH3$^+$	92.6 ± 0.7	0.18 ± 0.01	0.04 ± 0.01	40%	90%
8NH3$^+$	103.0 ± 0.4	0.19 ± 0.01	0.07 ± 0.01	36%	86%
2NH$_3^+$ 2COO$^-$	92.7 ± 0.4	0.23 ± 0.01	0.04 ± 0.01	33%	88%
4NH$_3^+$ 4COO$^-$	104.9 ± 0.4	0.22 ± 0.01	0.05 ± 0.01	44%	87%
4OH	92.2 ± 0.4	0.18 ± 0.01	0.03 ± 0.01	47%	91%
8OH	92.0 ± 0.6	0.22 ± 0.02	0.04 ± 0.01	36%	88%
4CONH$_2$	91.6 ± 0.6	0.21 ± 0.02	0.06 ± 0.01	35%	85%
8CONH$_2$	91.2 ± 0.7	0.21 ± 0.02	0.06 ± 0.01	38%	82%
3 × (2NH3$^+$)	88.7 ± 0.6	0.18 ± 0.02	0.02 ± 0.01	32%	95%
3 × (4NH3$^+$)	92.7 ± 1.2	0.10 ± 0.02	0.03 ± 0.01	59%	94%

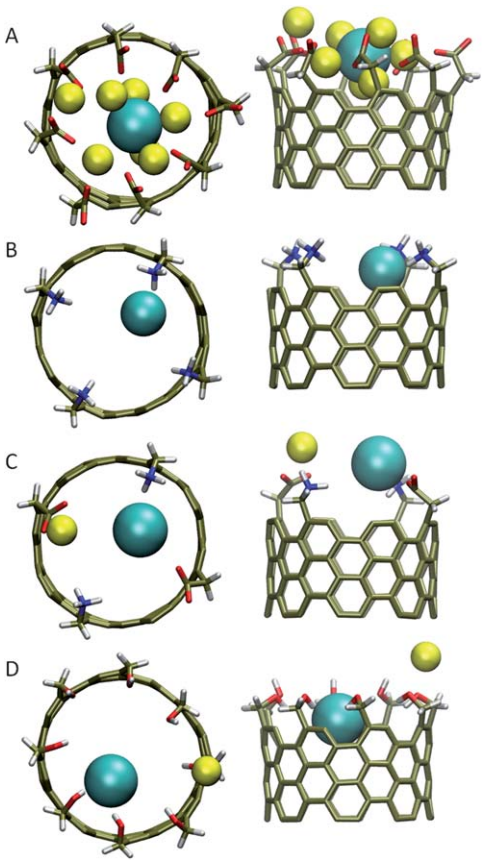

Fig. 4 Location of ions near the pore mouths. Side and top views of representative snapshots from MD simulations are shown to indicate the location and buildup of Na^+ (yellow) and Cl^- (blue) ions around the entrances of the functionalised CNTs. Results are shown for CNTs with (A) 8 COO^-, (B) 4 NH_3^+, (C) 2 NH_3^+ & 2 COO^- and (D) 8 OH groups respectively.

Table 4 Distribution of ions in the simulations. The average number of ions in the region of the pore mouth defined as $r < 6$ and $4.5 < z < 10.5$ as well as the average concentration in a 20 Å wide layer on each side of the membrane are given

	No. ions at mouth		Upstream (mM)		Downstream (mM)	
Tube type	Na^+	Cl^-	$[Na^+]$	$[Cl^-]$	$[Na^+]$	$[Cl^-]$
non func	0.07	0.07	317	324	91	81
$4COO^-$	0.64	0.00	360	275	119	90
$8COO^-$	3.43	0.65	450	251	78	64
$2NH_3^+$	0.04	0.24	319	369	77	85
$4NH_3^+$	0.09	1.23	295	387	71	84
$8NH_3^+$	0.00	1.73	237	439	72	99
$2NH_3^+$ $2COO^-$	0.32	0.24	325	325	92	94
$4NH_3^+$ $4COO^-$	0.30	0.04	337	348	87	82
4OH	0.12	0.18	315	326	95	87
8OH	0.20	0.18	314	323	96	87
$4CONH_2$	0.06	0.03	329	321	91	99
$8CONH_2$	0.23	0.04	335	337	79	87
$3 \times (2NH_3^+)$	0.05	0.26	313	363	80	86
$3 \times (4NH_3^+)$	0.00	1.05	249	553	45	78

Table 1, like charged ions are prevented from entering the pore due to electrostatic repulsions, creating valence selectivity in a manner similar to many biological channels.[33] Oppositely charged ions, however, build up at the entrance of the pore as shown in Fig. 4A. This in turn can create two issues: (i) a high conductance of that counter ion through the pore (and thus less efficient salt rejection) or (ii) the blockage of water molecules as described earlier. The inclusion of eight negative charges does prevent both ion types from passing. In this case the counter ions (Na^+) become trapped by the strong attraction to the mouth of the pore which can be seen in the energy well at this position in the Na^+ PMF (Fig. 6A). The depth of this energy well is not as great as may be expected considering the large number of negative charges that are present. In fact, the presence of multiple Na^+ ions tends to counteract the attraction to the charged groups, reducing the depth of the energy well. When only four

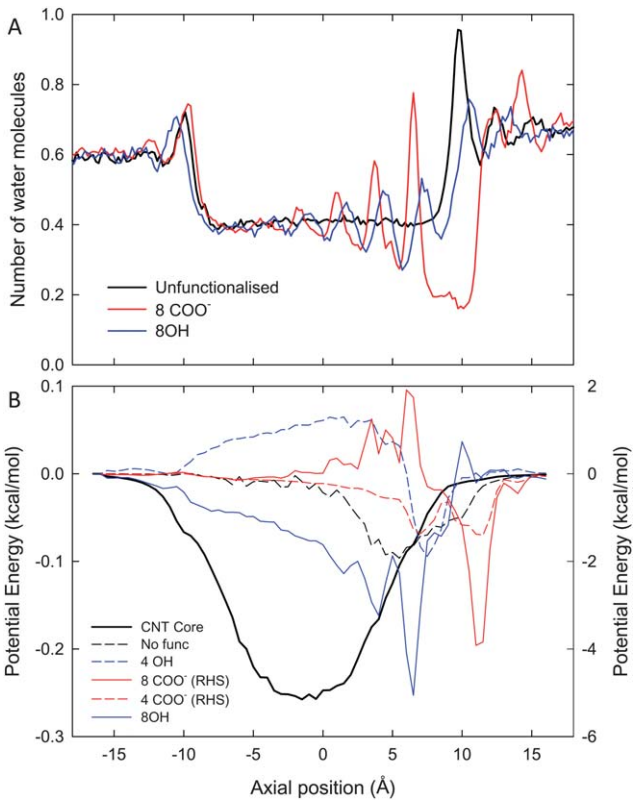

Fig. 5 Concentration profiles and interaction energies of water in the CNTs. (A) A one dimensional plot of the number of water molecules in 0.2 Å wide layers in the pores are shown for an unfunctionalised CNT (black), a CNT with 8 COO^- groups (red) and CNT with 8 OH groups (blue). (B) The interaction energy of water with the CNTs averaged over 8ns of simulation is shown as function of the position of the oxygen atom in the pore. The interaction with all but the end ring of carbon atoms, that is common to all the CNTs studied is shown by the thick black line. The average potential energy for interactions with the unfunctionalised end carbon ring (thin black line), the ring of 4 OH groups (dashed blue line) and 8 OH groups (solid blue line) are also shown with the energy values given by the left hand scale. The potential energy for interactions with the charged COO^- groups is much larger and is shown by the right hand scale for the case of 4 COO^- groups (dashed red line) and $8COO^-$ groups (solid red line).

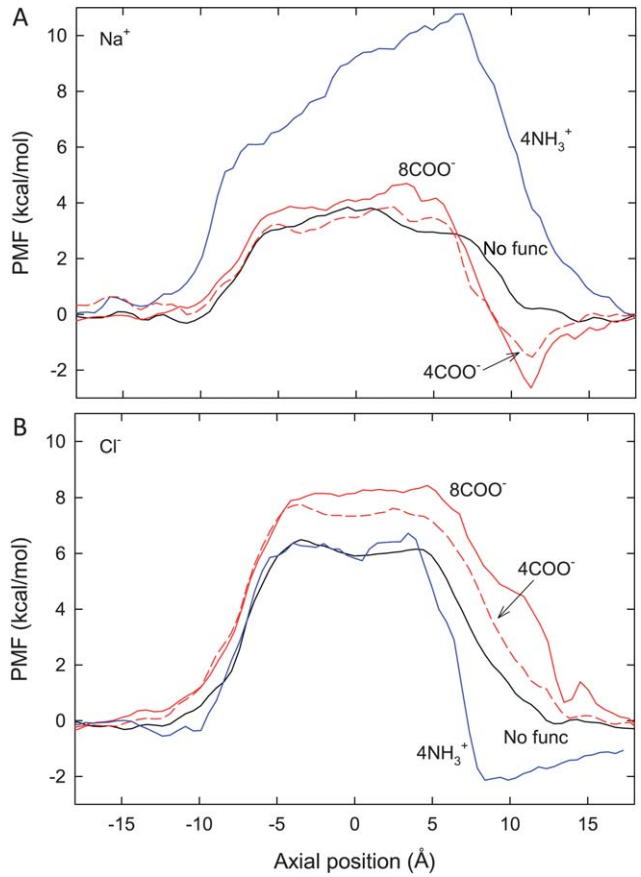

Fig. 6 Potential of mean force for ions in the pore. The 1D PMF is shown for (A) Na^+ and (B) Cl^- in an unfunctionalised CNT (solid line), CNT with 8 COO^- (red solid line), 4 COO^-(red dashed line) and 4 NH_3^+ (blue line).

charged groups are included the occasional presence of multiple Na^+ ions is enough to allow them to escape the electrostatic attraction of the COO^- groups and pass through the pore. The addition of four positively charged NH_3^+ groups is effective in rejecting both Na^+ and Cl^-. As shown in Fig. 6, Na^+ is strongly repelled from the pore mouth while Cl^- becomes temporarily trapped near the entrance, and thus faces a larger barrier to move into the interior of the pore than it does in the unfunctionalised CNT.

When both NH_3^+ and COO^- groups are added in equal measure to keep neutrality, the build up of ions at the pore entrance is less pronounced as seen in Table 4. The best results in the class with regard to water flux and salt rejection arise when just two NH_3^+ and two COO^- are included. Although both Na^+ and Cl^- ions are seen to remain fairly constantly near the channel entrance (Fig. 4C), the prevention of multiple ions of each type residing in this area means that both ions see a significant energy well and thus neither conducts through the channel at a large rate. The presence of these ions does, however, create significant steric hindrance to the passage of water which can be expected to reduce the water flux.

Another possible functionality is to add uncharged but polar groups at the channel entrance which may slow the motion of ions without holding them permanently near the channel mouth. To this end the effect of adding either OH or $CONH_2$ groups at the pore entrance was examined. Although ions did not reside around the channel mouth as commonly as seen in the other cases (Table 4), this did not act to prevent the ions from passing through the pore. Indeed, the addition of 4 OH groups actually assisted the passage of Na^+ relative to water. Although including a larger number of polar groups appeared to prevent the passage of Cl^-, none of the cases studied significantly increased the rejection of Na^+. The addition of the OH or $CONH_2$ groups also significantly slowed the permeation of water, due primarily to the increased electrostatic attraction of water to the pore.

Another issue worth considering is whether the density of functionalised CNTs in the membrane will influence either the water flux or salt rejection. Although only one of the 12 CNTs forming the membrane is functionalised in these simulations, due to the periodic nature of the simulation this actually represents a density of functionalised CNTs of 4.8×10^{16} pores m^{-2} which is greater than the CNT densities achieved in current membranes. At this density, neighbouring functionalised tubes are approximately 50 Å apart. Under most conditions this distance will be much greater than the Debye length of the electrolyte and the electrostatic field of each CNT will be screened out. Thus, neighbouring functionalised CNTs are unlikely to influence each other. Indeed, when desalinating sea water, interactions with neighbours can be expected to be screened out in under 10 Å ie when the density is less than 2×10^{17} pores m^{-2}.

If the functionalised CNTs are closer, however, then the transport in one tube may be influenced by the presence of the neighbour. In particular, this could be expected to be important when the CNTs are functionalised with charged groups in which case a greater density of charge could act to reject ions through charge repulsion. To examine this possibility simulations were conducted for two additional cases in which 3 neighbouring CNTs (labelled a, b and c in Fig. 1B) were all functionalised with either 2 or 4 NH_3^+ groups. It can be seen in Table 4 that the presence of 3 functionalised tubes decreases the concentration of Na^+ on the upstream side of the membrane when compared to the corresponding simulation with only one functionalised tube. Thus one would expect a greater Na^+ rejection due to charge repulsion. Simulations with only one tube functionalised with 4 NH_3^+ groups already showed 100% Na^+ rejection which cannot be further improved. But in the case of tubes functionalised with only 2 NH_3^+ groups, the presence of multiple functionalised CNTs close together did slightly improve Na^+ rejection. In reality, it is unlikely that functionalised CNTs will be able to be packed together as closely as described here, and if the supporting matrix is uncharged then it is the charge per tube, rather than the surface charge density that is likely to be most important for determining the salt rejection. The simulations with varying numbers of NH_3^+ groups do indicate that there is a minimum charge per CNT of around +4e required to effectively block Na^+.

4 Application to desalination technology

Having examined the water flux and ion rejection in a variety of functionalised (8,8) CNTs it is possible to reach some likely conclusions with regard to the effectiveness of functionalising CNTs in order to improve their performance in reverse osmosis membranes.

Functionalisation of the CNTs does influence salt rejection. The rejection of Cl^- is easier to achieve than that of Na^+ due to the inherently greater dehydration energy required for it to enter the pore. Thus, the inclusion of negatively charged groups or a number of polar groups effectively prevents Cl^- from permeating the pore. Preventing the smaller Na^+ from passing through the pore appears more difficult and was only achieved by the inclusion of positive charges at the entrance to repel the ion, or a very large number of negative charges that trap passing ions. Only two of the tubes examined were able to achieve complete rejection of both ion types: that with eight negative COO^- groups and that with four positive NH_3^+ groups, although the pores with a mixture of charged groups or with only 2 NH_3^+ groups show some improvement compared to the unfunctionalised tubes.

The obvious downside of CNT functionalisation is that it removes the smooth neutral pore surface that is responsible for the large flow of water through the pore, and thus the water flux is reduced in all cases studied. Whether this decreased flux is an impediment to using functionalised CNTs in desalination technology depends on how these fluxes compare to existing reverse osmosis membranes. Such a comparison is difficult for two reasons. Firstly, the performance of a CNT based membrane will be critically dependent on the density of pores that can be embedded in the supporting matrix. In these simulations the pores are packed side by side achieving the maximal possible pore density of around 5.8×10^{17} pores m^{-2}. In reality, achieving such a density is unlikely as the CNTs will need to be supported, but existing studies have reported pore densities as high as 2.5×10^{15} pores m^{-2}.[9] The second, and greater, difficulty arises from the fact that the small size and periodicity of the simulation systems being utilised makes it hard to accurately reproduce the build up of ions on one side of the membrane. Such concentrated layers are known to arise in reality, and are seen to some extent in these simulations. As shown in Fig. 1A a greater number of ions accumulate on the upstream side of the membrane than on the downstream side. This effect is quantified in Table 4 where the concentration of ions on each side of the membranes in each simulation is shown. On average these simulations show a concentration difference of about 3 : 1 across the membrane. While this represents a significant ion buildup, the concentration difference across desalination membranes can be expected to be even greater as ideally the downstream concentration will be less than 5% of that on the upstream side. Furthermore, the concentrated layer of ions is also likely to become more pronounced as the friction of the membrane is reduced, and thus leads to an eventual limit on the desalination efficiency that can be obtained,[34] which will be lower than that seen here. Given that this second fact is hard to account for completely in the simulated flow rates, the comparison here is limited to that based on the effective resistance of the pore to water with this roughly 3 : 1 concentration difference.

The water flux found in each of the functionalised tubes is given in macroscopic units in Table 2 assuming two different pore densities representing the maximum theoretical pore density and that achieved in laboratory scale CNT membranes.[9] Also shown is a rough decision on whether the desired salt rejection can be achieved with each functionality. As described previously, the permeability of the unfunctionalised (8,8) CNT membrane to water under hydrostatic pressure is between 20 and 5000 times that seen in the FilmTech SW30HR-380 commercial reverse osmosis membranes from Dow Water and Process Solutions[35] depending on whether the previously obtained, or maximum theoretical pore density is used. The osmotic permeability is also about 15 times greater than that seen in the water selective Aquaporin-1 channel.[36]

Even though the functionalised CNTs have a smaller water flux than the unfunctionalised tube, the flux assuming the lower pore density is still greater than the SW30HR-380 RO membrane. Under the conditions of these simulations, it would appear that all of these tubes could offer an improvement over current generation membranes in terms of water flow. Functionalising with 2 to 4 NH_3^+ groups, or 8 COO^- could also lead to near complete salt rejection.

The best compromise between water flux and salt rejection probably arises for narrower unfunctionalised CNTs. A 9.3 Å diameter (7,7) CNT, for example, can block over 95% of Na^+ and Cl^- ions yet has a water flux of around 60% that of the unfunctionalised (8,8) CNT.[20,21] The difficulty in synthesising or selecting only such narrow CNTs, however, will mean that larger diameter tubes may have to be used in the manufacture of novel reverse osmosis membranes. The results presented here indicate that in these cases chemical modification of the ends of the tubes may aid in improving salt rejection while still achieving water flows that are better than the current generation of polymer membranes. In reality, once the CNTs are uncapped as required for incorporation into filtration membranes, their ends are are likely to be chemically modified. For example COO^- groups are commonly reported to be present in such uncapped CNTs after oxidative cutting[10] and thus ideal non functionalised tubes may be a computational fantasy. This further emphasises that understanding the influence of such functionalisation on the potential use of CNTs in desalination membranes is extremely important for developing this technology.

Acknowledgements

This work was supported by funding from the National Health and Medical Research Council of Australia, the Australian Research Council, an award under the Merit Allocation Scheme on the NCI National Facility at the ANU, and computer time from iVEC.

References

1 I. A. Shiklomanov and J. C. Rodda. *Water Resources at the Beginning of the 21st Century*. Cambridge University press, 2003.
2 World Water Assessment programme. *The United Nations World Water Development Report 3: Water in a Changing World*. UNESCO and Earthscan, 2009.
3 *World Development Report 2010: Development and Climate Change*. The World Bank, 2010.
4 G. Hummer, J. C. Rasiah and J. Nowortya, Water conduction through the hydrophobic channel of a carbon nanotube, *Nature*, 2001, **414**, 188–190.
5 A. Kalra, S. Garde and G. Hummer, Osmotic water transport through carbon nanotube membranes, *Proc. Natl. Acad. Sci. USA*, 2003, **100**, 10175–10180.
6 A. I. Kolesnikov, J. M. Zanotti, C. K. Loong, P. Thiyagarajan, A. P. Moravsky, R. O. Loutfy and C. J. Burnham, Anomalously soft dynamics of water in a nanotube: A revelation of nanoscale confinement, *Phys. Rev. Lett.*, Jul 2004, **93(3)**, 035503.

7 N. Naguib, H. Ye, Y. Gogotsi, A. G. Yazicioglu, C. M. Megaridis and M. Yoshimura, Observation of water confined in nanometer channels of closed carbon nanotubes, *Nano Lett.*, 2004, **4**, 2237–2243.
8 B. J. Hinds, N. Chopra, T. Rantell, R. Andrews, V. Gavalas and L. G. Bachas, Aligned multiwalled carbon nanotube membranes, *Science*, 2003, **303**, 62–65.
9 J. K. Holt, A. Noy, T. Huser, D. Eaglesham and O. Bakajin, Fabrication of a carbon nanotube-embedded silicon nitride membrane for studies of nanometer-scale mass transport, *Nano Lett.*, 2004, **2**, 2245–2250.
10 M. Majumder, N. Chopra, R. Andrews and B. J. Hinds, Nanoscale hydrodynamics: Enhanced flow in carbon nanotubes, *Nature*, 2005, **438**, 44.
11 A. I. Skoulidas, D. M. Ackerman, J. K. Johnson and D. S. Sholl, Rapid transport of gases in carbon nanotubes, *Phys. Rev. Lett.*, 2002, **89**, 185901–185904.
12 F. Fornasieroa, H. G. Park, J. K. Holt, M. Stadermanna, C. P. Grigoropoulosc, A. Noya and O. Bakajin, Ion exclusion by sub-2-nm carbon nanotube pores, *Proc. Natl. Acad. Sci. USA*, 2008, **105**, 17250–17255.
13 O. Beckstein and M. S. P. Sansom, Liquid–vapor oscillations of water in hydrophobic nanopores, *Proc. Natl. Acad. Sci. USA*, 2003, **100**, 7063–7068.
14 R. Allen, J.-P. Hansen and S. Melchionna, A molecular dynamics investigation of water permeation through nanopores, *J. Chem. Phys.*, 2003, **119**, 3905–3919.
15 O. Beckstein and M. S. P. Sansom, The influence of geometry, surface character, and flexibility on the permeation of ions through biological pores, *Phys. Biol.*, 2004, **1**, 42–52.
16 A. Anishkin and S. Sukharev, Water dynamics and dewetting transitions in the small mechanosensitive channel MscS, *Biophys. J.*, 2004, **86**, 2883–2895.
17 M. Sotomayor and K. Schulten, Molecular dynamics study of gating in the mechanosensitive channel of small conductance, *Biophys. J.*, 2004, **87**, 3050–3065.
18 B. Corry, An energy-efficient gating mechanism in the acetylcholine receptor channel suggested by molecular and brownian dynamics, *Biophys. J.*, 2006, **90**, 799–810.
19 O. Beckstein and M. S. P. Sansom, A hydrophobic gate in an ion channel: the closed state of the nicotinic acetylcholine receptor, *Phys. Biol.*, 2006, **3**, 147–159.
20 B. Corry, Designing carbon nanotube membranes for efficient water desalination, *J. Phys. Chem. B*, 2008, **112**, 1427–1434.
21 C. Song and B. Corry, Intrinsic ion selectivity of narrow hydrophobic pores, *J. Phys. Chem. B*, 2009, **113**, 7642–7649.
22 T. A. Hilder, D. Gordon and S. H. Chung, Salt rejection and water transport through boron nitride nanotubes, *Small*, 2009, **5**, 2183–2190.
23 M. Majumder, N. Chopra and B. J. Hinds, Effect of tip functionalization on transport through vertically oriented carbon nanotube membranes, *J. Am. Chem. Soc.*, 2005, **127**, 9062–9070.
24 F. Zhu and K. Schulten, Water and proton conduction through carbon nanotubes as models for biological channels, *Biophys. J.*, 2003, **85**, 236–244.
25 A. D. MacKerell Jr., D. Bashford, M. Bellott, R. L. Dunbrack Jr., J. D. Evanseck, M. J. Field, S. Fischer, J. Gao, H. Guo, S. Ha, D. Joseph-McCarthy, L. Kuchnir, K. Kuczera, F. T. K. Lau, C. Mattos, S. Michnick, T. Ngo, D. T. Nguyen, B. Prodhom, W. E. Reiher III, B. Roux, M. Schlenkrich, J. C. Smith, R. Stote, J. Straub, M. Watanabe, J. Wiórkiewicz-Kuczera, D. Yin and M. Karplus, All-atom empirical potential for molecular modelling and dynamics studies of proteins, *J. Phys. Chem. B*, 1998, **102**, 3586–3616.
26 F. Zhu, E. Tajkhorshid and K. Schulten, Pressure-induced water transport in membrane channels studied by molecular dynamics, *Biophys. J.*, 2002, **83**, 154–160.
27 F. Zhu, E. Tajkhorshid and K. Schulten, Theory and simulation of water permeation in aquaporin-1, *Biophys. J.*, 2004, **86**, 50–57.
28 G. M. Torrie and J. P. Valleau, Monte carlo free energy estimates using non-Boltzmann sampling: Application to the sub-critical Lennard-Jones fluid, *Chem. Phys. Lett.*, 1974, **28**, 578–581.
29 S. Kumar, D. Bouzida, R. H. Swendsen, P. A. Kollman and J. M. Rosenberg, The weighted histogram analysis method for free energy calculations on biomolecules.1. the method, *J. Comput. Chem.*, 1992, **13**, 1011–1021.
30 B. Roux, The calculation of potential of mean force using computer simulations, *Comput. Phys. Commun.*, 1995, **91**, 275–282.
31 Alan Grossfield. An implementation of WHAM: the Weighted Histogram Analysis Method. http://membrane.urmc.rochester.edu/Software/WHAM/WHAM.html (accessed 26/1/2010).
32 J. C. Phillips, R. Braun, W. Wang, J. Gumbart, E. Tajkhorshid, E. Villa, C. Chipot, R. D. Skeel, L. Kale and K. Schulten, Scalable molecular dynamics with NAMD, *J. Comput. Chem.*, 2005, **26**, 1781–1802.
33 B. Corry and S. H. Chung, Mechanisms of valence selectivity in biological ion channels, *Cell Mol. Life Sci.*, 2006, **63**, 301–315.
34 M. A. Shannon, P. W. Bohn, M. Elimelech, J. G. Georgiadis, B. J. Mariñas and A. M. Mayes, Science and technology for water purification in the coming decades, *Nature*, 2008, **452**, 301–310.
35 Dow water and process solutions. http://www.dowwaterandprocess.com/products/membranes/sw30hr_380.htm (accessed 22/9/2010).
36 A. B. Mamonov, R. D. Coalson, M. L. Zeidel and J. C. Mathai, Water and deuterium oxide permeability through Aquaporin 1: MD predictions and experimental verification, *J. Gen. Physiol.*, 2007, **130**, 111–116.